

Surface modification of optical materials with hydrogen plasma for fabrication of Bragg gratings

ULIANA O. SALGAEVA,¹ ANATOLIY B. VOLYNCEV,¹ AND SERGIO B. MENDES^{2,*}

¹Physics Department, Perm State National Research University, Perm 614068, Russia

²Department of Physics and Astronomy, University of Louisville, Louisville, Kentucky 40292, USA

*Corresponding author: sbmend01@louisville.edu

Received 28 October 2015; revised 2 December 2015; accepted 9 December 2015; posted 10 December 2015 (Doc. ID 252824); published 13 January 2016

We investigate the hydrogen plasma process as a route for creating Bragg gratings (BGs) on optoelectronic materials such as undoped lithium niobate (LiNbO_3), proton-exchanged LiNbO_3 , and soda-lime glass. Photopatterns (periodic modulations, $\Lambda = 323\text{--}2000$ nm) were created on those substrates and the hydrogen plasma process was investigated for its ability to transfer the microstructures and the underlying mechanisms involved in this process. The diffraction efficiency and surface topology of the BG were characterized, as well as the optical properties of corresponding bulk materials undergoing the same plasma treatment. It is shown that the hydrogen plasma treatment changes the complex refractive index and modifies the surface topology with a volume expansion in the near-surface region, and both features are connected to the appearance of structural defects in the materials. The hydrogen plasma offers unique flexibility and advantages that can be explored for the fabrication of integrated photonic components. © 2016 Optical Society of America

OCIS codes: (220.4000) Microstructure fabrication; (130.3120) Integrated optics devices; (230.1950) Diffraction gratings.

<http://dx.doi.org/10.1364/AO.55.000485>

1. INTRODUCTION

Increasing attention has been paid to plasma treatments for tailoring the properties of optical materials in desired ways. There are a large number of physical and chemical processes that can be carried out under a plasma environment, and the performance of each process significantly depends on the gas composition, processing conditions, and the composition and structure of the material under treatment. Hydrogen plasma presents an interesting approach to the conventional plasma approaches due to the high mobility of hydrogen atoms and associated ions that can easily penetrate inside a material structure creating complex effects on the surface and near-surface regions of the substrate which can lead to changes in the material's physical and chemical properties. Like many plasma processes, the hydrogen plasma treatment is a good alternative for processes involving wet chemistry, high pressure, high temperature, and others. There have been a few reports on the applications of hydrogen plasma treatment. For example, work by Ren and others [1,2] aimed to substitute the standard proton-exchange process of LiNbO_3 crystals performed with acids (e.g., benzoic, adipic, stearic, and other well-known proton donors) with a treatment in hydrogen plasma for the fabrication of optical waveguides. Other reports have shown the possibility

to form in the near-surface a layer of chemically reduced LiNbO_3 using treatments with hydrogen and oxygen plasmas [3,4]. Both reports describe a decrease in the optical transmission and an increase in the surface roughness of LiNbO_3 substrates. It is interesting to note that similar changes have been shown in amorphous fused silica substrates after treatment with hydrogen plasma [5].

Therefore, it is relevant to investigate why materials with crystal and amorphous structures demonstrate similar behaviors under the influence of the hydrogen plasma treatment and to understand the physical and/or chemical mechanisms that are responsible for such properties. In this article, we show that the hydrogen plasma process creates substantial changes in the structural physical properties and in the surface topology of several relevant materials for optoelectronic applications—soda-lime glass, undoped LiNbO_3 , and proton-exchanged (PE) LiNbO_3 substrates. Our in-depth and solid investigation of those features has provided us the opportunity to demonstrate for the first time (to the best of our knowledge) the fabrication of Bragg gratings (BGs) on the surface of those optical materials using the hydrogen plasma process. The choice of these materials is based on their high availability and performance for fabrication of integrated optical circuits.

For thorough investigations on the properties of the BGs and the corresponding bulk materials under the same plasma treatment, methods of optical spectrophotometry, atomic force microscopy, and diffraction efficiency in the Littrow configuration were deployed and their experimental results are shown in this report.

2. EXPERIMENT

A. Sample Preparation

For our experiments, we used slides of soda-lime glass ($25\text{ mm} \times 76\text{ mm} \times 1\text{ mm}$), X-cut slides of LiNbO_3 ($15\text{ mm} \times 40\text{ mm} \times 1\text{ mm}$), and PE LiNbO_3 ($15\text{ mm} \times 40\text{ mm} \times 1\text{ mm}$) substrates. Proton-exchanged LiNbO_3 samples were fabricated with a closed metal reactor process using undiluted benzoic acid $\text{C}_6\text{H}_5\text{COOH}$ at $T = 174^\circ\text{C}$ for 2 h and then annealed at $T = 354^\circ\text{C}$ in air for 300 min [6].

Samples were cleaned, spin-coated with a photoresist film (Microposit, Shipley S1805), exposed to laser light (He–Cd, 442 nm laser line) using a holographic technique based on two-beam interference from a Lloyd's mirror configuration [7] (Fig. 1), and developed (Microposit, Shipley 351) for creation of a periodic pattern in the photoresist layer [Figs. 2(a)–2(c)].

Additional details of this process have been described by us and can be found elsewhere [7]. Bragg diffraction gratings with periodic modulation from 323 to 2000 nm were fabricated on different samples. For a series of experiments, a hard-metal mask was required. For this purpose, a 20 nm layer of aluminum was deposited over the periodic pattern created in the photoresist layer (with periods ranging from 500 to 2000 nm) and then a lift-off process of the photoresist material was performed by

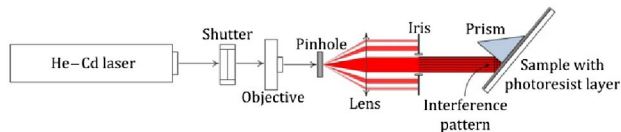


Fig. 1. Schematic representation of the Lloyd's mirror configuration for the holographic exposure and creation of periodic photopatterns.

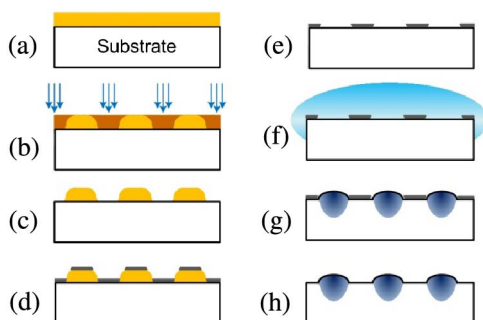


Fig. 2. Sample preparation procedure: (a) coating with photoresist, (b) holographic interference exposure, (c) photopattern development, (d) Al layer deposition, (e) lift-off in solvent, (f) H-plasma treatment, (g) sample after plasma treatment, and (h) sample after removal of photopattern mask.

sonication of the substrates in acetone or N-dimethylformamide to form a periodic metallic pattern [Figs. 2(d)–2(e)].

For the purpose of investigating the structural changes due to the hydrogen plasma treatment in both the periodic-structured regions as well as in large opened areas of the substrate material, we have covered with kapton tape the back surface of each sample and removed the mask layer from selected regions of the front surface of the substrate. A schematic representation of the fabricated sample is presented in Fig. 3.

B. Treatment in Hydrogen Plasma

Samples with a periodic photopattern, either in photoresist or a metal layer as described above and shown in Figs. 2 and 3, were loaded in a plasma reactor (quartz tube) of a capacitively coupled plasma (CCP) source shown in Fig. 4. Prior to plasma generation, the reactor was evacuated up to 0.5 Torr. Pure hydrogen was used as a process gas with a typical flow rate through the system of 15.0 ± 0.5 sccm. For generation of plasma with high density, the power of the CCP source was set in the range of 25–100 W at a frequency of 13.4 MHz. The samples were placed in a region inside the quartz tube surrounded by the split-ring electrode system (charged and grounded electrodes). The time duration of the plasma treatment varied from 30 to 120 min for different samples. In order to provide an extra flexibility in the sample treatment process, an additional heating was supplied by enclosing the sample with a tube furnace placed near the plasma generation region. For samples with a photoresist mask layer, the additional heating was not applied and the temperature of the tube furnace was controlled not to exceed 80°C as to prevent any hard-baking of the photoresist or

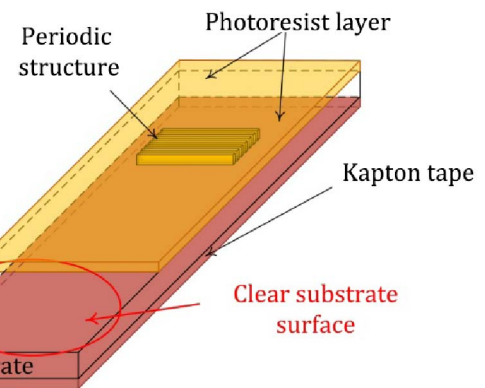


Fig. 3. General schematic of the sample with a photoresist mask prepared for plasma treatment.

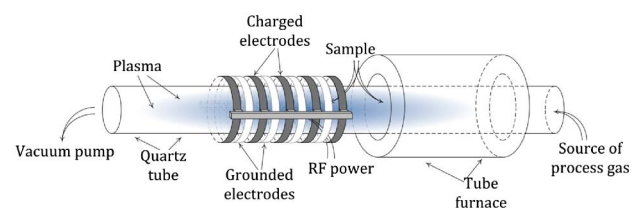


Fig. 4. View of the CCP source used for carrying out the hydrogen plasma treatments.

Table 1. Treatment Conditions of the Samples in Hydrogen Plasma

No.	Material	Mask	Λ , nm	t , min	P , W	T , °C	Diffraction efficiency, %	Surface modulation, nm	ΔT at 633 nm, %
1	Glass	S1805	323	30	50	-	$10^{-5}(S)$	1-2	0.7
2	Glass	S1805	1000	60	50	75 ± 5	$5 \times 10^{-5}(P)$	5	1.0
3	Glass	Al	2000	120	45	300 ± 5	$1.5(S)$	90	1.9
4	LiNbO ₃	S1805	350	30	50	-	$5 \times 10^{-5}(P)$	1-2	1.5
5	LiNbO ₃	Al	1000	60	75	150 ± 5	$6.4 \times 10^{-4}(P)$	80	2.6
6	LiNbO ₃	Al	1000	150	50	200 ± 5	$0.13(S)$	30	4.0
7	PE:LiNbO ₃	S1805	350	30	50	-	$10^{-5}(S)$	n/a	n/a
8	PE:LiNbO ₃	S1805	2000	60	50	80 ± 5	$10^{-4}(S)$	4-5	15.72
9	PE:LiNbO ₃	Al	1000	60	50	250 ± 5	$0.04(S)$	2-3	66

mask degradation under the influence of temperature and hydrogen plasma. Samples with an Al mask layer were treated at higher temperatures 120°C–300°C. Data with the conditions of plasma treatment for different samples are shown in Table 1.

After the plasma treatment, the photoresist masks were removed with sequential sonication during 10 min in a piranha solution (1:3 of hydrogen peroxide to sulfuric acid) at 60°C and then 10 min in acetone; the metal mask was removed with sonication in 0.3% NaOH solution until removing all Al film from the sample surface.

After the treatment of hydrogen plasma and removal of the mask layer from the substrates, diffraction efficiency measurements and surface topology characterizations were performed for the regions of the fabricated periodic structures. Also, optical transparency was measured for the large area of each substrate that was also exposed to the plasma treatment.

C. Diffraction Efficiency

Measurement of diffraction efficiency is important to characterize periodic structures as it provides a direct and nondestructive assessment of the changes in the structural and optical properties of the material undergoing plasma treatment. It is expected that the hydrogen plasma can induce changes in the refractive index (Δn) of the treated substrates, similar to what happens in the proton-exchange process. It is also possible that structural modifications may occur in the topology of the exposed surfaces during the plasma process. The magnitude of those changes should depend directly on the intensity and conditions of the plasma process. When we compare the diffraction efficiency of BG devices with the same pitch size and probed under the same Littrow configuration with the same light polarization and wavelength, the diffraction efficiency will be able to report the magnitude of the periodic modulations transferred to the optical substrates during the plasma process. Therefore, measurements of the diffraction efficiency of BGs provide a nondestructive although indirect estimation of the efficiency of the hydrogen plasma process for modulating the physical and chemical properties of the substrate material.

For diffraction efficiency measurements, a He–Ne laser (632.8 nm) was deployed as the light source and a Littrow configuration was setup for each grating period [7], which is schematically shown in Fig. 5. The results for those measurements are shown in Table 1 (data tabulated for the *S*- or *P*-polarized light for the negative first-order of diffracted light in transmission, T_{-1}). Considering that diffraction efficiency depends on

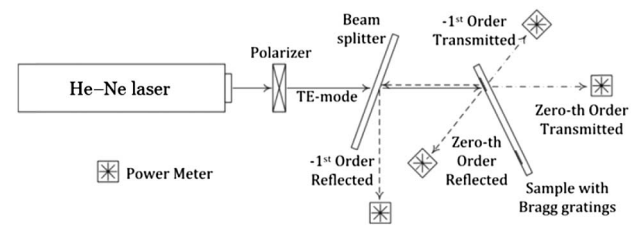


Fig. 5. Schematic representation of the experimental configuration deployed for the characterization of diffraction efficiency of our samples.

the pitch size of the periodic structure (Λ), material characteristics, and light polarization, the comparative should be restricted to those similar conditions. The results summarized in Table 1 show that the diffraction efficiency of the periodic structures fabricated with the plasma process increases with a higher power of the plasma source, a longer time of treatment, and a higher temperature of the additional annealing. The diffraction efficiency of BG fabricated on PE:LiNbO₃ substrate is consistently much higher than the diffraction efficiency of a similar BG formed on the surface of pristine LiNbO₃ crystals. Glass substrates exhibit lower diffraction efficiency when compared to similar BGs formed in LiNbO₃ materials.

For BG samples fabricated without any additional heating (up to 100°C), a performance reduction on the diffraction efficiency was observed over time. This decrease in performance occurred during several days after the plasma treatment until it leveled off at a certain minimum value. This minimum value was about 10 times smaller than the diffraction efficiency measured in the first day of treatment (and listed in Table 1). It is important to note that, after achieving this minimum value, the diffraction efficiency of those samples no longer changed (for an observation time window of about 1 year) or at least the changes are negligible and occur at nondetectable rates. On the other hand, for samples treated with additional heating in the hydrogen plasma, the rates of diffraction efficiency of fabricated periodic structures remain remarkably the same (even 6 months after treatment).

D. Surface Topology

Experimental results obtained by different research groups [1–4] report on changes of surface roughness of LiNbO₃ due to hydrogen plasma treatment. In this work, the surface

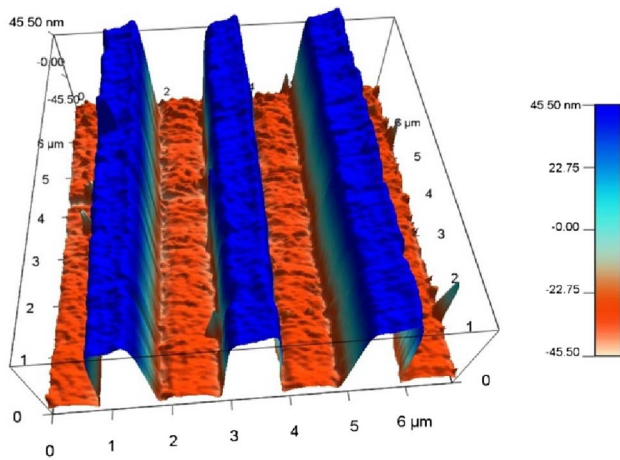


Fig. 6. Periodic pattern produced by the H-plasma treatment of a glass substrate processed through an Al mask ($\Lambda = 2000$ nm) during 120 min with an additional heating of 300°C . The higher elevations in the periodic structure (blue) correspond to the regions exposed to the plasma process and the troughs (red) correspond to those regions originally protected by the Al photopattern. Data collected after removal of the Al photopattern.

topology of our samples were investigated with an atomic force microscope (AFM probe from Oxford Instruments, Asylum MF3D) after the mask layer deployed during the plasma treatment has been removed. AFM measurements were performed at regions of the sample where a periodic mask was originally located and at large and open regions of the sample that were also exposed to the same plasma treatment. Figure 6 shows the AFM topography of a glass sample for a region treated through the periodic mask layer.

At first glance, one may consider that such kind of plasma treatment would cause etching of the regions subjected to the

influence of the hydrogen plasma environment and consequently the creation of a periodic pattern. However, careful analysis of the exposed and unexposed regions on the sample surface showed a swelling of the region subjected to the influence of the hydrogen plasma. The regions exposed to the plasma process (open grooves in the original mask layer structure) showed a higher elevation of the surface topology with a clear increase in height compared to the regions that were protected by the grating grooves. Therefore, the main mechanism for the creation of the periodic pattern was determined to be not an etching process but rather an expansion of the surface topology. The transferred pattern to the substrate is thus a negative one compared to the mask structure. We also observed that when tougher plasma conditions were applied to the samples, a more pronounced effect was measured on the microrelief patterns. Additional evidence of the phenomenon is illustrated in Fig. 7 for a LiNbO_3 sample. This effect was observed in all treated samples of soda-lime glass, LiNbO_3 , and PE: LiNbO_3 with heights on the microrelief pattern ranging from several to one hundred nanometers. It is also important to notice that the topology of the periodic microrelief structure of the BGs also decreased with time for those samples that a decrease in diffraction efficiency was observed (data not shown here).

E. Optical Transmittance and Changes in the Complex Refractive Index

As demonstrated above, the hydrogen plasma process created an elevated structure on the treated regions of the substrate. However, it is also quite possible that it may create a graded structure that can tailor the complex refractive index on those same regions exposed to the plasma process. To access those effects, measurements of the refractive index were carried out using both spectrophotometric and prism-coupler techniques.

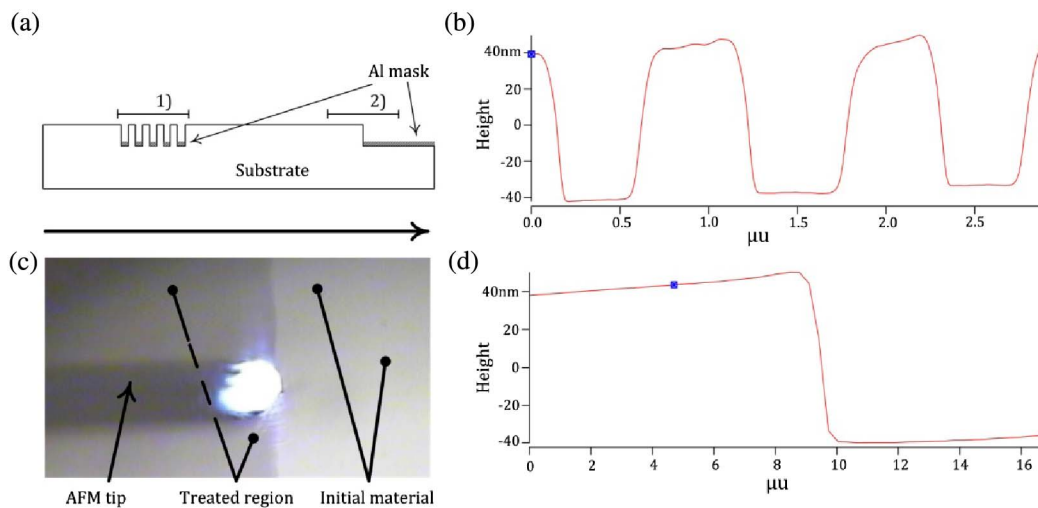


Fig. 7. AFM investigation of a LiNbO_3 sample treated under hydrogen plasma at 150°C during 60 min. (a) Schematic representation of a sample region (1) corresponding to the BG produced through an Al photopattern ($\Lambda = 1000$ nm), and region (2) corresponding to an open area on the substrate and treated in plasma and initial (covered with Al mask) substrate. (b) AFM profile of the BG at region (1) with an 80 nm height difference between the upper grooves (exposed) and lower troughs (originally covered with the Al mask). (c) A photographic picture of the region mapped by the AFM measurements, where the darker area corresponds to the exposed region (2) shown in part (a). The AFM scanning was carried out from the left to the right side. (d) Profile of region (2) shown in (a) with an 80 nm height difference between treated (higher part) and initial (lower part). Data collected after removal of the Al photopattern.

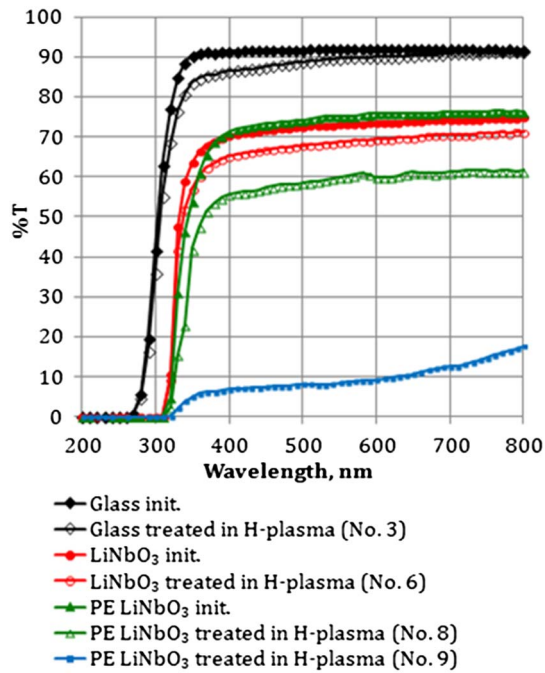


Fig. 8. Measurements of optical transmittance for substrates before (init.) and after treatment in hydrogen plasma at different processing conditions (sample number corresponds to the row in Table 1).

In case the hydrogen plasma treatment could create a higher refractive index compared to the original substrate and could reach diffusion lengths that were comparable to the light wavelength, then prism-coupler measurements would allow us the determination of the effective refractive indices of the waveguide modes and their comparison with the refractive index of the untreated bulk material. A number of attempts were undertaken with the prism-coupling approach (Metricon, 2010/M) to detect refractive index changes between the treated and untreated regions; however, those changes were not detected, which most likely are due to the shallow depth of the plasma processed structures.

After treatment in hydrogen plasma, changes in color and optical transparency of the processed substrates (soda-lime glass, LiNbO_3 , PE:LiNbO_3) could be observed with the naked eye. Soda-lime glass became yellowish after treatment, LiNbO_3 and PE:LiNbO_3 samples gained a color from light gray to black. Spectrophotometric measurements (Varian, Cary 300) of optical transmittance for untreated samples and treated samples in the hydrogen plasma of soda-lime glass, LiNbO_3 , and PE:LiNbO_3 substrates are shown in Fig. 8. The stronger the plasma conditions were applied during the treatment (higher temperature and/or higher power of the plasma source), the higher the reduction in optical transmittance was observed.

3. DISCUSSION

As demonstrated by our experimental results, the hydrogen plasma treatment of optical materials such as soda-lime glass, pristine LiNbO_3 , and PE:LiNbO_3 can be used for the fabrication of BGs with pitch size, Λ , from 323 to 2000 nm using periodic masks formed either in photoresist or a metal layer. This

type of application of the hydrogen plasma treatment is shown for the first time, to the best of our knowledge. The working principle of the fabricated periodic optical structures is based not only on the organized periodic microrelief structures created on the surface of the optical materials but also on the periodic modulation of the complex refractive index of the top structure of the substrate. Particularly important are the changes in the imaginary part of the refractive index (also known as the extinction coefficient) as shown by the reduction in the optical transmittance of samples after the hydrogen plasma treatment.

Several causes can be acting to decrease the optical transmittance of the LiNbO_3 and PE:LiNbO_3 substrates: (i) chemical reduction of LiNbO_3 (formation of NbO compound characterized with a darkening color) during the hydrogen plasma treatment, as was indicated in previous reports [1,3], (ii) a weak proton-exchange process [1], (iii) formation of F^- and F^+ color centers in the near-surface of the substrate region [1,3], and (iv) formation of additional kinds of structural and radiation-induced defects initialized by electrons, UV radiation, and hydrogen ions (H , H^+ , H^- , H_2 , H_2^+ , H_3^+) that may penetrate and diffuse into the material and change its properties. The last mechanism (iv) is also considered to be relevant for the reduction of the optical transmittance in soda-lime glass.

Another interesting outcome of the investigated process is the swelling of the optical materials on the regions exposed to the hydrogen plasma treatment, where the surface topology was characterized with elevations ranging from 1 to 100 nm depending on plasma treatment conditions. Although a small increase in surface roughness was associated with such process previously [1], this kind of topology change was not precisely detected, quantified, and correlated with the plasma processing conditions. The fabricated Bragg grating devices allowed us to precisely detect and quantify those features. The observed swelling of the structures can be explained as a result of defect formation and lattice expansion in the optical materials. Our data show that this kind of lattice modification should have a shallow depth (less than 1 μm) because a change in the refractive index, which usually goes along with a change in the lattice constant, was not detected by our deployed optical methods. Moreover, previous experiments [1] showed data confirming the assumption about a shallow depth for a modified-surface layer with hydrogen plasma treatment. It was detected that hydrogen from the plasma environment penetrates to the LiNbO_3 substrate not deeper than 1 μm . Because of the similar optical results that were measured in the investigated optical materials, it is likely that comparable depths for the hydrogen penetration are occurring in the soda-lime glass substrates.

It is also relevant to notice that the effect of decreasing the diffraction efficiency and surface modulation over time for a class of BG devices (those fabricated in hydrogen plasma without the essential additional heating) can be explained on the basis of dynamics of the structural defects in solid-state materials. As time passes, the structural defects formed during the plasma treatment relax and/or plasma-injected hydrogen ions diffuse from energetically unfavorable positions to more favorable lattice vacancies.

As a side note, it may be relevant to mention our observation that the hydrogen plasma process is significantly affected by the

presence of kapton tape during the plasma treatment. Most likely, the out-gassing of the kapton tape under the hydrogen plasma environment can prevent a strong chemical reduction (blackening) of the LiNbO_3 substrate. As a consequence, sample 9 in Table 1 (and other samples not presented in the Table 1) shows a strong reduction in optical transmittance after the plasma process. As can be observed in Table 1, sample 9 has a relatively low surface modulation of about 2–3 nm but it is able to provide a detectable diffraction efficiency due to the strong optical changes from the plasma process. This illustrates the roles played by both the microrelief formation and the changes in complex refractive index toward the creation of the BG structures under the hydrogen plasma process.

4. CONCLUSIONS

The modification of relevant optical materials by the hydrogen plasma process with the formation of a surface layer with an altered complex refractive index and an elevated topology has been investigated and thoroughly characterized. By combining those features with photopatterning techniques we have demonstrated the fabrication of periodic modulations on the optical substrates for the development of BG devices with the hydrogen plasma treatment. The underlying process has several physical and chemical mechanisms which span from the interaction of charged particles with the substrate material, the penetration and diffusion of those into the structure, and formation of lattice defects and chemical reactions. The underlying dynamics induces simultaneous appearance of changes in the surface topology and in the complex refractive index at the near-surface region of the optical material, and both components can contribute and be adjusted to the formation of photonic devices. The hydrogen plasma process described here provides for the possibility of fabricating devices with adjustable surface and index contrast, and those features are expected to

bring additional resources and flexibility for developing several optical components such as Bragg grating filters in integrated photonic circuits, integrated grating couplers, phase plates, and dispersive diffraction gratings.

Funding. Ministry of Education of Perm Territory (C-26/004.02); National Institutes of Health (NIH) (RR022864); National Science Foundation (NSF) (0814194); Kentucky Science and Energy Foundation (KSEF) (1869-RDE-012).

REFERENCES

1. Z. Ren, P. J. Heard, K. R. Hallam, A. Wotherspoon, Q. Jiang, R. Varrazza, and S. Yu, "Fabrication and characterizations of proton-exchanged LiNbO_3 waveguides by inductively coupled plasma technique," *Appl. Phys. Lett.* **88**, 142905 (2006).
2. Z. Ren, P. J. Heard, and S. Yu, "Proton exchange and diffusion in LiNbO_3 using inductance coupled high density plasma," *J. Vac. Sci. Technol. B.* **25**, 1161–1165 (2007).
3. H. Turcicova, J. Vacik, J. Cervena, V. Perina, M. Polcarova, J. Bradler, V. Zelezny, and J. Zemek, "LiNbO₃ exposed to radio-frequency plasma," *Nucl. Instrum. Methods Phys. Res. B* **141**, 494–497 (1999).
4. H. Turcicova, H. Arend, and O. Jarolimek, "A low-resistance layer on LiNbO_3 produced in hydrogen RF discharge," *Solid State Commun.* **93**, 979–981 (1995).
5. C. Gerhard, D. Tasche, S. Bruckner, S. Wieneke, and W. Viol, "Near-surface modification of optical properties of fused silica by low-temperature hydrogenous atmospheric pressure plasma," *Opt. Lett.* **37**, 566–568 (2012).
6. S. S. Mushinsky, A. M. Minkin, I. V. Petukhov, V. I. Kichigin, D. I. Shevtsov, L. N. Malinina, A. B. Volyntsev, M. M. Neradovskiy, and V. Ya. Shur, "Water effect on proton exchange of x-cut lithium niobate in the melt of benzoic acid," *Ferroelectrics* **476**, 84–93 (2015).
7. C. M. Hayes, M. B. Pereira, B. C. Brangers, M. M. Aslan, R. S. Wiederkehr, S. B. Mendes, and J. H. Lake, "Sub-micron integrated grating couplers for single-mode planar optical waveguides," in *University/Government/Industry Micro/Nano Symposium UGIM 17th Biennial (IEEE, 2008)*, pp. 227–232.